pubs.acs.org/environau

Atrazine Degradation Using Immobilized Triazine Hydrolase from Arthrobacter aurescens TC1 in Mesoporous Silica Nanomaterials

Karla Diviesti, Glory A. Russell-Parks, Brian G. Trewyn, and Richard C. Holz*



Downloaded via COLORADO SCHOOL OF MINES on November 16, 2023 at 21:27:43 (UTC). See https://pubs.acs.org/sharingguidelines for options on how to legitimately share published articles.

Cite This: ACS Environ. Au 2023, 3, 361-369



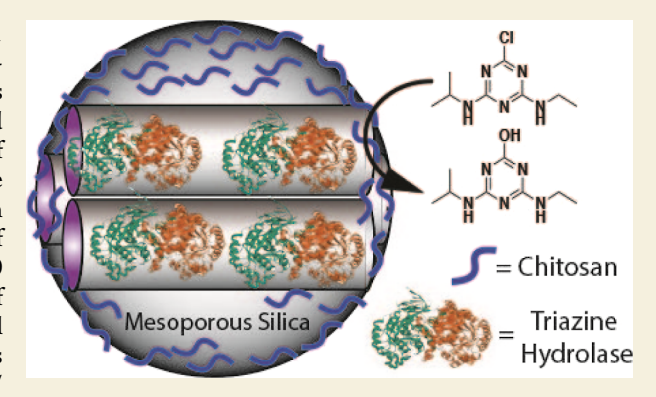
ACCESS I

Metrics & More

Article Recommendations

s Supporting Information

ABSTRACT: Triazine hydrolase from *Arthrobacter aurescens* TC1 (TrzN) was successfully immobilized on mesoporous silica nanomaterials (MSNs) for the first time. For both nonfunctionalized MSNs and MSNs functionalized with Zn(II), three pore sizes were evaluated for their ability to immobilize wild-type TrzN: Mobile composition of matter no. 41 (small, 3 nm pores), mesoporous silica nanoparticle material with 10 nm pore diameter (MSN-10) (medium, 6–12 nm pores), and pore-expanded MSN-10 (large, 15–30 nm pores). Of these six TrzN:MSN biomaterials, it was shown that TrzN:MSN-10 was the most active ($3.8 \pm 0.4 \times 10^{-5}$ U/mg) toward the hydrolysis of a 50 μ M atrazine solution at 25 °C. The TrzN:MSN-10 biomaterial was then coated in chitosan (TrzN:MSN-10:Chit) as chitosan has been shown to increase stability in extreme conditions such as low/



high pH, heat shock, and the presence of organic solvents. TrzN:MSN-10:Chit was shown to be a superior TrzN biomaterial to TrzN:MSN-10 as it exhibited higher activity under all storage conditions, in the presence of 20% MeOH, at low and high pH values, and at elevated temperatures up to 80 °C. Finally, the TrzN:MSN-10:Chit biomaterial was shown to be fully active in river water, which establishes it as a functional biomaterial under actual field conditions. A combination of these data indicate that the TrzN:MSN-10:Chit biomaterial exhibited the best overall catalytic profile making it a promising biocatalyst for the bioremediation of atrazine.

KEYWORDS: zinc, dehalogenase, biomaterials, kinetics, mesoporous silica nanoparticles, biocatalysis, bioremediation

1. INTRODUCTION

Originally patented in 1958 in Switzerland, atrazine (2-chloro-4-ethylamino-6-isopropylamino-s-triazine) has been used commercially in the United States (US) since 1959, and today, it is the second most applied herbicide, with ~30,000 tons annually to sorghum, sugar cane, and corn crops. 1-3 Atrazine is water-soluble and functions to inhibit photosynthesis in targeted plants but is an environmental contaminant of streams, rivers, and groundwater. It is persistent and mobile in aquatic environments, primarily through surface runoff, where it gets into groundwater via leaching. Its ability to enter and move through these environments after application is troublesome due to the potential downstream effects, particularly given its half-life of 6 months to several years and its toxicity to many eukaryotes such as crustaceans, insects, mollusks, fish, amphibians, and reptiles. 1,4-6 The documented effects of atrazine on lower-order eukaryotes raise concerns for possible toxicity to humans. Links have been shown between atrazine exposure and lung and kidney diseases, cardiovascular damage, retinal degeneration, and cancer, which is why in 2003 the European Union banned atrazine. In the US, the environmental protection agency recognized atrazine as an endocrine toxin in humans. Given the widespread use of atrazine in the US and its toxicity to both aquatic environments and humans, its biodegradation and environmental remediation have become a topic of significant importance.⁸

Triazine hydrolase from *Arthrobacter aurescens* TC1 (TrzN, EC 3.8.1.8) is a Zn(II)-dependent hydrolytic dehalogenase that catalyzes the conversion of atrazine to its less toxic derivative hydroxyatrazine under physiological conditions (Scheme 1). Converting atrazine to hydroxyatrazine is considered the most efficient way to decrease atrazine contamination in the environment; therefore, TrzN is the biocatalyst of choice for the production of biomaterials that can be used in the bioremediation of atrazine contamination. Bioremediation methods utilizing TrzN, to date, have been limited to whole cells that naturally express TrzN or in one case, simply adding pure TrzN to a contaminated drainage ditch.^{8,9} While these were somewhat successful in atrazine

Received: July 7, 2023
Revised: October 5, 2023
Accepted: October 6, 2023
Published: November 1, 2023





Scheme 1. Hydrolysis of Atrazine to Hydroxyatrazine by TrzN

$$\begin{array}{c|c} CI & OH \\ \hline N & N & H_2O & H^+ + CI^- \\ \hline N & H & H \end{array}$$

bioremediation, purified TrzN immobilized on a support material is necessary as a major challenge is the recovery of whole cells or free enzymes from the environment. In addition, within a cell, side reactions pose challenges with competing metabolic pathways and the toxicity of the substrate and/or products. Recently, some of us demonstrated that TrzN could be successfully immobilized within alginate and tetramethylorthosilicate (TMOS) sol—gels that function as effective biocatalysts for atrazine degradation. Although effective, the response of sol—gel biocatalysts tends to be limited and slow due to diffusion limitations. In addition, depending on the procedure used to prepare these systems, there can be gradual leaching over time. 12

Mesoporous silica nanomaterials (MSNs) provide a promising platform for the entrapment of enzymes, offering enhanced stability, improved catalytic activity, and protection against harsh environmental conditions. 13 These unique materials possess an ordered pore structure with well-defined pore sizes and high surface areas, which is ideal for immobilizing enzymes. Not only does the porous nature of mesoporous silica facilitate the diffusion of substrates and products, allowing efficient enzyme-substrate interactions, but also these materials are highly tunable, so they can accommodate various enzymes as well as substrates. 14,15 Moreover, the surface chemistry of these nanomaterials can be easily modified, enabling tailored immobilization strategies and enhanced enzyme loading. For example, various metal ions are commonly incorporated within MSNs which promote a covalent interaction to occur between the metal ion and a protein tag. Although metal ions such as Cu²⁺, Ni²⁺, and Co²⁺ can be utilized, there is a trade-off between the specificity and affinity of the interaction between the metal ion selected and the protein tag. 16 For this work, we functionalized our material(s) with Zn2+ ions to covalently tether TrzN through its N-terminus histidine (His) tag allowing for increased stability in comparison to the noncovalent protein-loaded materials. The Zn²⁺/His-tag chelation is a highly used bioconjugation as there is a strong affinity for the imidazole group within the His-tag. 17 Therefore, TrzN was immobilized within MSNs (noncovalently and covalently), providing a novel biocatalytic nanomaterial that is capable of the hydrolytic degradation of atrazine under mild conditions.

2. MATERIALS AND METHODS

2.1. Materials

Chitosan, atrazine, type I trypsin from the bovine pancreas, and chymotrypsin were purchased from Sigma-Aldrich. Triblock copolymer Pluronic P104 (PEO $_{27}\mbox{PPO}_{61}\mbox{PEO}_{27})$ was received as a gift from BASF. Millipore nanopure water was filtered at 18.2 $\mbox{M}\Omega.$ All reagents were of the highest purity available and were obtained without further purification.

2.2. Synthesis of Mobil Composition of Matter No. 41 (MCM-41; Pore Size of ~3 nm)

The commonly reported procedure was followed to synthesize MCM-41. Briefly, 1.0 g of cetyltrimethylammonium bromide was added to 480 mL of nanopure water followed by the addition of 3 mL of NaOH (2.0 M). The mixture was stirred for 30 min at 80 °C and 4.6 g of tetraethylorthosilicate was then added dropwise, and the mixture was allowed to stir for an additional 2 h. The opaque solution was then filtered and washed with nanopure water and ethanol three times, each with the final wash being ethanol. The white material was dried overnight in air. The crude product was then dispersed in methanol (25 mL), and a small volume of concentrated HCl was added (250 μ L). This was stirred for 6 h at 64 °C, which promoted the removal of the surfactant. The material was again filtered, washed with ethanol, and dried overnight.

2.3. Synthesis of Mesoporous Silica Nanoparticle Material with 10 nm Pore Diameter (MSN-10; Pore Size of 6–12 nm)

A 3.5 g portion of a nonionic surfactant, Pluronic P104, was dissolved in 1.6 M HCl at 55 $^{\circ}$ C for 1 h. 5.1 g of TMOS was then added dropwise, and the mixture was further stirred for 24 h at 55 $^{\circ}$ C. During this time, the solution changed from a clear, colorless solution to a white mixture. This mixture was transferred to a Teflon-lined autoclave and was hydrothermally treated at 150 $^{\circ}$ C for 24 h. Next, the mixture was cooled, filtered, and washed three times with both water and methanol, with the final wash being methanol, leaving a white solid. Finally, the powder was dried overnight and then calcined at 550 $^{\circ}$ C for 6 h to remove the surfactant. ¹⁹

2.4. Synthesis of Pore-Expanded MSN-10 (Pore Size of 15-30 nm)

The same procedure used to synthesize the MSN-10 material was followed except that 8.4 g of 1,2,4,5-tetramethylbenzene was added dropwise to the solution to swell the pores after P104 had dissolved. This mixture was then stirred for an additional 1 h at 55 °C before TMOS was added. After hydrothermal treatment, washing, and drying the material, an acid extraction was performed to remove the surfactant. Here, the crude pore-expanded material was added to a solution consisting mainly of methanol (115 mL) and a small volume of concentrated HCl (2.3 mL), which was then refluxed for 6 h. The product was filtered and washed with water and methanol two times each and dried overnight in air.

2.5. Zn-Functionalized MSN-10

Zinc was incorporated within the MSN by following the published procedure. 20 A solution of the previously synthesized MSN-10 (1.0 g) dispersed in nanopure water (8.0 mL) was prepared, along with a second solution consisting of $\rm Zn(NO_3)_2$ (0.2 g) dissolved in nanopure water (2.0 mL). Initially, while raising the pH of the Zn solution to 11, the addition of NH₄OH caused a precipitate to form; however, after further addition of NH₄OH, the solution returned to a clear, colorless solution. Once the pH of both solutions had been adjusted to 11, the Zn solution was quickly added with stirring to the MSN-10 mixture. After stirring for 10 min, the solid material was separated via centrifugation (10 min). Nanopure water (8 mL) was added to the solid material which was then allowed to stir for an additional 10 min. The material was then filtered and washed with water three times and dried overnight. Lastly, the material was calcined at 300 °C for 3 h.

2.6. Material Characterization

All MSN materials were characterized by the following techniques: nitrogen physisorption analysis at 77 K using a Micromeritics TriStar 3000. A 20 s equilibration time was used to obtain the isotherms of each material. From these isotherms, the specific surface area and pore distribution of the samples were extracted through the Brunauer–Emmett–Teller (BET) equation and the Barrett–Joyner–Halenda (BJH) method; scanning transmission electron microscopy (STEM) images and the corresponding energy-dispersive X-ray spectroscopy (EDS) hypermaps were collected on a FEI Talos F200X operated at 200 kV. The samples were suspended in methanol and dropped onto

a 300-mesh copper grid with lacey Formvar/carbon (Ted Pella, 01883-F). Elemental EDS maps were both collected (acquisition time 5 min) and processed by standard methods using Bruker ESPRIT software; powder X-ray diffraction (pXRD) was performed on a Bruker D2 Phaser diffractometer with Cu $K\alpha$ (λ = 1.54 Å) with a current of 10 mA and a voltage of 30 kV; inductively coupled plasma atomic emission spectroscopy (ICP–AES) analysis was performed on a PerkinElmer Optima 8300; thermogravimetric analysis (TGA) was performed using a TA Instruments TGA Q500 with the internal high-resolution programming ramping to 800 °C at a ramp rate of 10 °C min⁻¹ in air; scanning electron microscopy (SEM) images were collected on a SEMTech Solutions Refurbished Amray 3300 field emission scanning electron microscope with an accelerating voltage of 15 kV and a working distance between 10 and 15 mm.

2.7. Expression and Purification of TrzN

The gene from A. aurescens TC1 that encodes for TrzN with the D38N, L131P, and A159V mutations was expressed and purified as previously reported.¹⁷ Briefly, a 100 mL Luria-Bertani (LB)-Miller starter culture was inoculated from a single colony with 50 $\mu g/mL$ of kanamycin. A 9 L culture was inoculated from this starter culture using 10 mL/liter supplemented with 5 μ M isopropyl β -D-1thiogalactopyranoside and grown at 37 °C for 48 h. 11,23 Cells were harvested by centrifugation at 7000 rpm at 4 °C for 15 min. The cells were resuspended at 2 mL per gram of buffer A (50 mM NaH₂PO₄, 500 mM NaCl, 10 mM imidazole, 1.5 mM tris(2-carboxyethyl)phosphine, 10% glycerol, pH 8.0) and then lysed by sonication on ice in three 10 min (30 s on, 45 s off) intervals using a 21 W Misonex sonicator 3000. Cell debris was removed by centrifugation at 17,500 rpm, 4 °C, for 40 min. The protein was purified by immobilized metal affinity chromatography (IMAC) using Ni-NTA (nickel-nitrilotriacetic acid) Superflow Cartridges (Qiagen). The column was equilibrated with buffer A, and the crude protein extract was loaded onto the IMAC column. Unbound protein was eluted with 15 column volumes (CV) of buffer A at a flow rate of 2 mL/min. Elution of TrzN was initiated with 15 CV of 3% buffer B (buffer A with 500 mM imidazole). The elution finished with a linear gradient (3-100%) of buffer B over 20 CVs at a flow rate of 2 mL/min. Peak fractions were pooled and resuspended in 50 mM [4-(2-hydroxyethyl)-1-piperazineethanesulfonic acid] HEPES at pH 7.5 and concentrated with an Amicon Ultra-15 centrifugal filter device with a molecular weight cutoff (MWCO) of 30,000 (Millipore). Sodium dodecyl sulfatepolyacrylamide gel electrophoresis reveals a single polypeptide band at ~51 kDa, consistent with previous studies (Figure S13, Supporting Information). ^{11,21,23} The protein concentration was determined by ultraviolet (UV)—vis absorbance at 280 nm ($\varepsilon_{280} = 61,670 \text{ M}^{-1} \text{ cm}^{-1}$) and with a Coomassie (Bradford) Protein Assay Kit (Thermo Scientific). Expression of TrzN and purification using IMAC resulted in ~10 mg/L of soluble TrzN enzyme. 11,21,23

2.8. Kinetic Activity Assay

Hydrolysis of atrazine by TrzN was quantified spectrophotometrically by continuously monitoring the decrease in absorbance at 264 nm ($\varepsilon_{264}=3.5~\mathrm{mM}^{-1}~\mathrm{cm}^{-1}$) that accompanies atrazine dechlorination, as previously reported. Briefly, the hydrolysis of a 150 $\mu\mathrm{M}$ atrazine solution in 0.1 M sodium phosphate buffer, pH 7.0, was monitored at 264 nm. Assays were performed in a 1 mL quartz cuvette in triplicate on an Agilent 8453 UV—vis spectrophotometer. One unit of enzyme activity was defined as the amount of enzyme that catalyzed the hydrolysis of 1 $\mu\mathrm{mol}$ of atrazine per minute at 25 °C. Plots of the initial rate of hydrolysis of various concentrations of atrazine were fit to the Michaelis—Menten equation, which provided a catalytic constant (k_cat) of 4.0 \pm 0.1 s $^{-1}$ and a Michaelis constant (k_m) value of 43 \pm 3 $\mu\mathrm{M}$, similar to those previously reported. 11,21,23

2.9. Immobilization of TrzN on MSNs in the Absence and Presence of a Chitosan Coating

TrzN was adhered to MSNs (5 mg) in 50 mM HEPES buffer, pH 7.0 (1.0 mL), followed by the addition of 2.5 mg of TrzN in 250 μ L of 50 mM HEPES buffer, pH 7.0. The TrzN:MSN mixture was placed on a shaker plate for 20 h at room temperature (160 rpm). The

TrzN:MSN biomaterial was then centrifuged (10 min), and the supernatant was separated from the solid material and the amount of protein loaded was quantified using a Coomassie (Bradford) Protein Assay Kit (Thermo Scientific). TrzN:MSN was also coated in chitosan by modifying and combining two previously published procedures. A 0.5% w/v chitosan solution was used and prepared in a 2% acetic acid solution at pH 6.0. The TrzN:MSN material (5 mg) was placed in 5 mL of the chitosan solution and stirred at 25 °C at 200 rpm for 24 h. After the coating process, the TrzN:MSN:chitosan biomaterial was separated by centrifugation at 4000 rpm at 20 °C for 10 min. The samples were washed with 50 mM HEPES buffer, pH 7.0, and allowed to air-dry for 30 min prior to being used.

2.10. Kinetic Characterization of the TrzN:MSN Biomaterials

Hydrolysis of atrazine by each TrzN:MSN biomaterial was determined using a 50 μ M atrazine solution in 50 mM HEPES pH 7.0 at 25 °C with constant stirring (200 rpm). ^{11,27} Aliquots of the reaction mixture (0.3 mL) were taken at fixed time intervals, and the hydrolysis of atrazine was analyzed via the UV—vis assay previously described for wild-type (WT) TrzN. The specific activity (U/mg) of each biomaterial was calculated from the reaction rate (μ mol/L/min), the amount of TrzN immobilized, and the volume of the reaction. ^{11,28} Reaction buffer (1 mL) was collected at the end of each reaction for protein loss analysis using a Coomassie Protein Assay Kit (Thermo Scientific). The concentration of atrazine produced was determined using standard curves of absorbance versus known atrazine concentrations.

2.11. Recycling Experiments for TrzN:MSN Biomaterials

A 5 mL solution of 50 μ M atrazine in 50 mM HEPES, pH 7.0, at 25 °C was reacted with each TrzN:MSN biomaterial for 1 h, after which an aliquot (1 mL) was removed and the amount of atrazine dechlorination determined via the UV-vis assay previously described for WT TrzN. The product mixture was then decanted, and the TrzN:MSN samples were stored in three post-reaction storage conditions: no buffer stored at -80 °C, no buffer stored at 4 °C, and 1 mL of HEPES buffer, pH 7.0, at 4 °C and reused on a weekly basis for 6 weeks. The reaction buffer was tested for protein loss from the MSN using a Coomassie (Bradford) Protein Assay Kit (Thermo Scientific). The reaction was also repeated on a different TrzN:MSN sample group over 6 cycles with each cycle using standard reaction times and the conditions described above. Samples of TrzN:MSN biomaterials were used for each cycle with no wash step in between cycles, and an aliquot (1 mL) of reaction buffer was taken after each cycle to evaluate protein loss using the Coomassie (Bradford) Protein Assay Kit (Thermo Scientific).

2.12. Activity of Soluble and Immobilized TrzN in Organic Cosolvents

The activity of soluble TrzN with 5, 10, and 20% (v/v) methanol as the organic cosolvent toward atrazine was measured spectrophotometrically at 25 $^{\circ}\text{C}$ as described above. Each measurement was performed in triplicate. The degradation of atrazine using each TrzN:MSN biomaterial with organic cosolvents at concentrations ranging from 5 to 100% (v/v) was carried out in their respective reaction conditions described previously. Aliquots (1 mL) were taken at the start and end of the reaction and analyzed spectrophotometrically as described above. After reacting with the cosolvent, samples were washed with 5 mL of 50 mM HEPES buffer pH 7.0, and the same sample was reacted again at the standard reaction time and conditions described previously.

2.13. Activity of Soluble and Immobilized TrzN at pH Values of 4 and 9

The activity of soluble and immobilized TrzN in 50 mM citric acid, pH 4.0 and 50 mM glycine buffer, pH 9.0, toward atrazine was measured spectrophotometrically as described above. Each measurement was taken in triplicate. Aliquots (1 mL) were taken at the end of the reactions and tested for protein loss using the Coomassie (Bradford) Protein Assay Kit (Thermo Scientific).

2.14. Thermostability of Soluble and Immobilized TrzN

The thermostability of soluble and immobilized TrzN was determined by incubating each for 30 min at 50, 60, 70, and 80 °C. Soluble TrzN was in 1 mL aliquots in 50 mM HEPES buffer, pH 7.0, while TrzN:MSN biomaterials were not suspended in buffer. The residual activity of the free enzyme and encapsulated TrzN was determined spectrophotometrically.

2.15. Activity of TrzN:MSN in Natural Water Samples

Water samples were collected on April 14th, 2023, from Clear Creek in Golden, Colorado. Temperature, pH, and metal analysis (using ICP–AES) were collected the same day. Aliquots (100, 200, and 300 μ L) were plated on agar plates and incubated for 48 h to detect general bacterial growth. Two sets of sample groups were tested from the Clear Creek samples; one group used autoclaved water samples and the other did not. Autoclaved samples were done prior to the addition of biocatalyst to ensure that there was no inactivation due to the autoclave process. The activity of the TrzN:MSN biomaterials was tested spectroscopically as described above. Aliquots (1 mL) were taken at the end of the reactions and tested for protein loss using the Coomassie (Bradford) Protein Assay Kit (Thermo Scientific).

3. RESULTS AND DISCUSSION

3.1. Material Characterization

The physical properties of the MSNs were examined by a series of characterization techniques. The calculated BET surface areas and BJH pore diameters from nitrogen sorption analysis, are shown in Table 1. These data demonstrate the successful

Table 1. Properties of Synthesized MSNs

sample	BET surface area (m^2/g)	pore diameter (nm)	pore volume (cm³/g)
MCM-41	968	3	1.26
MSN-10	397	9	1.14
PEMSN-10	321	21	2.46
Zn@MCM-41	736	2.5	0.857
Zn@MSN-10	358	9	1.14
Zn@PEMSN-10	293	15	1.52
chitosan MSN-10	225	9	0.685

synthesis of three different pore-sized MSN materials. The physical properties of the nonfunctionalized MSN materials are characteristic of these types of MSNs and are consistent with previous reports. ¹⁹ After functionalization with Zn(II), a decrease in surface area was observed, indicating the incorporation of Zn(II). A decrease in surface area and pore volume was also observed for MSN-10 coated with chitosan, suggesting that the coating procedure was successful. Type IV isotherms, which are characteristic of mesoporous materials, were maintained after Zn(II) functionalization and chitosan coating (Figures S1–S4, Supporting Information). The steep slope at low P/P₀ observed with the MCM-41 sample is indicative of micropore filling caused by the presence of enhanced adsorbent—adsorptive interactions. ²⁹

Transmission electron microscopy (TEM) analysis of MSN-10 shows the hexagonal particle morphology and ordered pore distribution of the unmodified material (Figure 1A). Elemental mapping reveals the presence and uniform dispersion of Zn(II) throughout the nanoparticle after functionalization (Figure 1B–D). STEM images of MCM-41 show that the particles are uniform in shape and size (Figure S5, Supporting Information), while STEM images of PEMSN-10 show porous, nonuniform particles. This material was deemed acceptable for this study as the desired pore properties were achieved

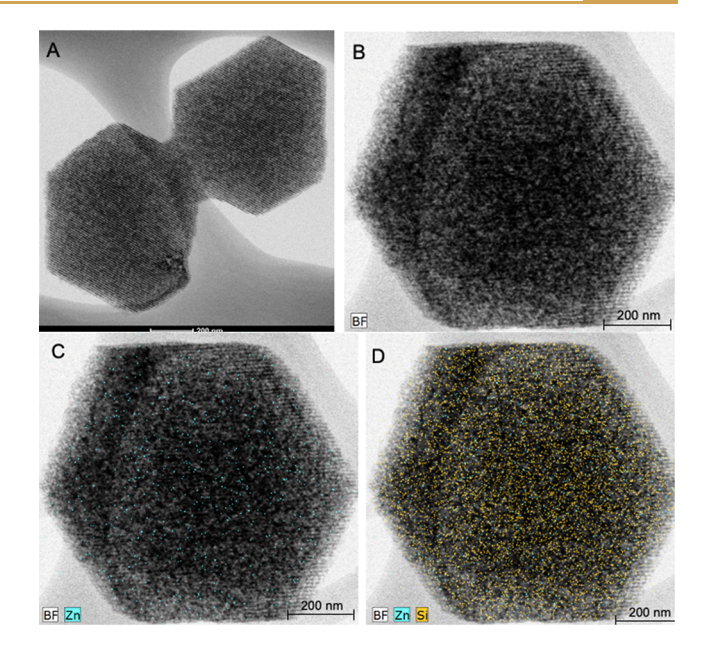


Figure 1. STEM images of nonfunctionalized (A) and Zn(II)-functionalized MSN-10 (B-D). Zn(II) is represented as blue, and Si is represented as yellow. The scale bar is 200 nm.

(Figure S6, Supporting Information). Elemental mapping of MCM-41 and PEMSN-10 materials also shows the dispersion and presence of Zn(II) (Figures S5 and S6, Supporting Information). These findings suggest that TrzN could be covalently tethered throughout the material (surface and pores, size permitting). The amount of Zn(II) incorporated into the materials was quantified by ICP-AES after digesting the solid materials in HF and aqua regia and diluting with 5 wt % HCl (Table S1, Supporting Information), further confirming the successful addition of Zn(II). The 100-peak observed at 2θ of 0.7° for the unfunctionalized MSN-10 in the low-angle pXRD analysis indicates ordered pores, which can also be observed in the STEM images (Figure S7, Supporting Information). After the addition of the chitosan coating, SEM images show that there are no changes to the particle morphology (Figure S8, Supporting Information). TGA was also performed, which revealed a mass loss at 180 °C in the presence of chitosan (Figure S9, Supporting Information).³⁰ The mass loss from the chitosan coating is low, which is expected, as we expect the coating to be thin.

3.2. Immobilization of TrzN

Purified WT TrzN catalyzed the hydrolysis of atrazine and exhibited a $k_{\rm cat}$ value of $4.0\pm0.1~{\rm s}^{-1}$ and a $K_{\rm m}$ value of 4.3 ± 3 $\mu{\rm M}$ at 25 °C in 50 mM HEPES buffer, pH 7.0, consistent with those previously reported. TrzN was incorporated onto nonfunctionalized MSNs, which lack direct, controlled chemical interactions for immobilizing enzymes within the pore framework as only silica surface interactions with amino acids of TrzN exist. To provide further stability of TrzN, the bare MSNs were functionalized with Zn(II) to encourage a covalent bond between the N-terminal His₆ affinity tag on TrzN and the Zn(II)-coated MSN surface. TEM images (Figure 1B) in addition to ICP analysis (see Supporting Information) demonstrate the successful incorporation of Zn(II) on the MSN surface.

For both functionalized and nonfunctionalized MSNs, three pore sizes were evaluated for their ability to immobilize 5 mg

of catalytically active, pure TrzN: MCM-41 (small, 3 nm), MSN-10 (medium, 6–12 nm), and PEMSN-10 (large, 15–30 nm) (Table 1, see Supporting Information for N_2 sorption isotherms, XRD, and ICP). For the small pore size, the nonfunctionalized MSN immobilized 37.1 \pm 0.4% of the TrzN, while the Zn(II)-functionalized MSN immobilized 99.6 \pm 0.2%. For the medium pore size, 24.2 \pm 0.3% of the protein was immobilized, while 98 \pm 0.1% of protein was immobilized for the Zn(II)-functionalized MSN. Lastly, the nonfunctionalized PEMSN-10 immobilized 36.7 \pm 0.0% of the protein, and the Zn(II)-functionalized form immobilized 99.2 \pm 0.1%. The protein loading was determined by calculating the change between the amount of protein in the loading buffer and the amount remaining after the immobilization step with a Coomassie (Bradford) Protein Assay Kit (Thermo Scientific).

Both the functionalized and nonfunctionalized Trzn:MSNs readily reacted with 50 μ M atrazine at 25 °C in 50 mM HEPES buffer, pH 7.0, over a 1 h reaction period. The observed activities were evaluated over 5 cycles (Figure 2). Activity

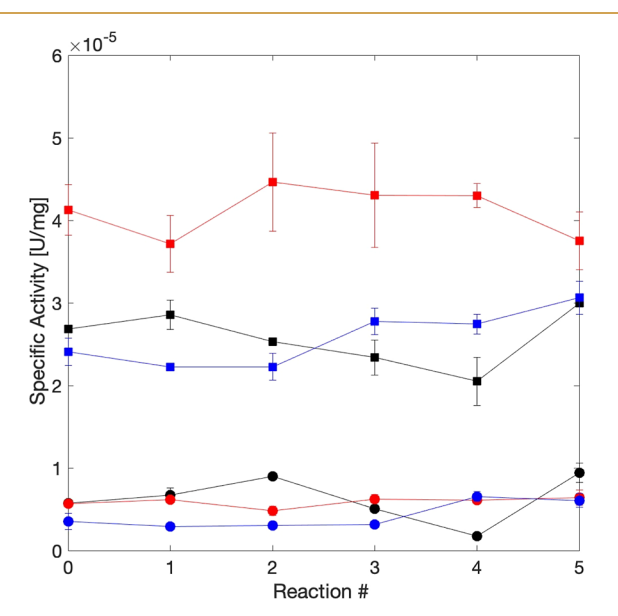


Figure 2. Five-cycle analysis, using specific activity U/mg, for the hydrolysis of 50 μ M atrazine at 25 °C in 50 mM HEPES buffer, pH 7.0, for 1 h. Using TrzN-loaded functionalized and nonfunctionalized MSNs: MCM-41 (small, 3–3.5 nm, black), MSN-10 (medium, 6–12 nm, red), and pore-expanded MSN-10 (large, ~15–30 nm, blue). The Zn(II)-functionalized TrzN:MSNs are denoted as circles, and the nonfunctionalized TrzN:MSNs are denoted as squares.

assays for the nonfunctionalized Trzn:MSNs revealed that the TrzN:MSN-10 biomaterial exhibited the highest specific activity at $3.8 \times 10^{-5} \pm 0.4 \times 10^{-5}$ U/mg after 5 cycles, while the TrzN:MCM-41 biomaterial exhibited a specific activity of $3.0 \times 10^{-5} \pm 0.9 \times 10^{-5}$ U/mg which was similar to the TrzN:PEMSN-10 biomaterials $3.1 \times 10^{-5} \pm 0.6 \times 10^{-5}$ U/mg. The higher observed activity for the TrzN:MSN-10 biomaterial suggests that 6–12 nm is the optimal pore size for TrzN immobilization. On the other hand, a clear trend emerged for the Zn(II)-functionalized MSNs, regardless of pore size, as every TrzN:MSN biomaterial exhibited significantly lower activity than the corresponding nonfunctionalized TrzN:MSN biomaterial (Figure 2). These data are at first surprising considering that increased activity is typically observed when enzymes are covalently attached;

however, after evaluating the electrostatic surface map of TrzN, a highly negative area was observed around the active site pocket (Figure S10, Supporting Information), suggesting that the active site is blocked due to binding to the Zn(II)-functionalized silica surface. Such a binding mode would be expected to inhibit substrate access to the TrzN active site. ^{31,32}

3.3. Immobilization of TrzN on MSNs with a Chitosan Coating

Chitosan is a derivative of chitin, the second most abundant cationic polymer in the world, and has a repeating structure of (1,4)-linked β -D-glucosamine.³³ When paired with biomaterials, chitosan has shown to increase stability in extreme conditions such as low/high pH, heat shock, and the presence of organic solvents. 11,34,35 Specifically, with MSN, chitosan has been used to enhance the efficacy of other catalysts used as delivery systems for drugs and therapeutics. 36,37 There is no or limited information available about studies using chitosancoated MSN for purposes beyond delivery, such as environmental remediation. As chitosan is permeable to the substrate, coating TrzN:MSN biomaterials with chitosan was hypothesized to provide additional protection for TrzN without inhibiting catalytic activity. Therefore, the TrzN:MSN-10 biomaterial was coated with chitosan (TrzN:MSN-10:Chit) and was shown to readily react with 50 μ M atrazine at 25 °C in 50 mM HEPES buffer, pH 7.0, over a 1 h reaction period with no detectable protein loss after the reaction (Figure 3).

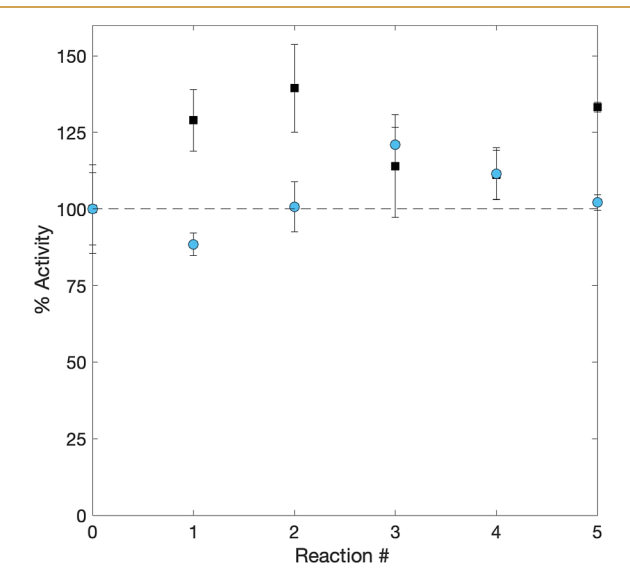


Figure 3. Cyclical reusability of TrzN:MSN-10 (black squares) and TrzN:MSN-10:Chit (light blue circles) evaluated over five cycles by monitoring the hydrolysis of 50 μ M atrazine at 25 °C in 50 mM HEPES buffer, pH 7.0, for 1 h. Each point represents five 1 h cycles with no wash step between cycles.

Compared to the TrzN:MSN-10 biomaterial, the TrzN:MSN-10:Chit biomaterial exhibited 94 \pm 4% of the activity, suggesting that the added coating had little to no effect on TrzN's ability to hydrolyze atrazine. These data indicate that both the TrzN:MSN-10 and TrzN:MSN-10:Chit biomaterials display the expected enzymatic properties, including substrate recognition, as WT TrzN in solution.

3.4. Reusability and Recycling of TrzN:MSN Biomaterials

For commercial applications, a biocatalyst must be reusable and have long-term stability. With this in mind, TrzN:MSN-10

and TrzN:MSN-10:Chit biomaterials were investigated under numerous reusability conditions. First, the biocatalysts were recycled multiple times in subsequent reactions (Figure 3). The materials were tested over five 1 h cycles with no wash step in-between cycles. Both materials retained full activity over five consecutive reactions with no quantifiable protein loss. Next, both biocatalysts were tested over a six-week period with three different storage conditions: dry (no buffer) at 4 °C, wet in 1 mL of 50 mM HEPES buffer, pH 7.0, at 4 °C, and dry at -80 °C. A wash step with 50 mM HEPES buffer, pH 7.0, was essential after every reaction to remove residual atrazine and hydroxyatrazine. Over the six-week period, the TrzN:MSN-10:Chit biomaterial outperformed the TrzN:MSN-10 biomaterial in all three storage methods. In the dry storage method at 4 °C (S11A, Supporting Information), TrzN:MSN-10 and TrzN:MSN-10:Chit retained 15 ± 11 and $59 \pm 2\%$ of their initial activity, respectively. In the -80 °C storage method (S11B, Supporting Information), TrzN:MSN-10 retained 39 \pm 7%, while TrzN:MSN-10:Chit retained 73 \pm 10% of their initial activity. Lastly, in the aqueous storage method (Figure 4), the TrzN:MSN-10

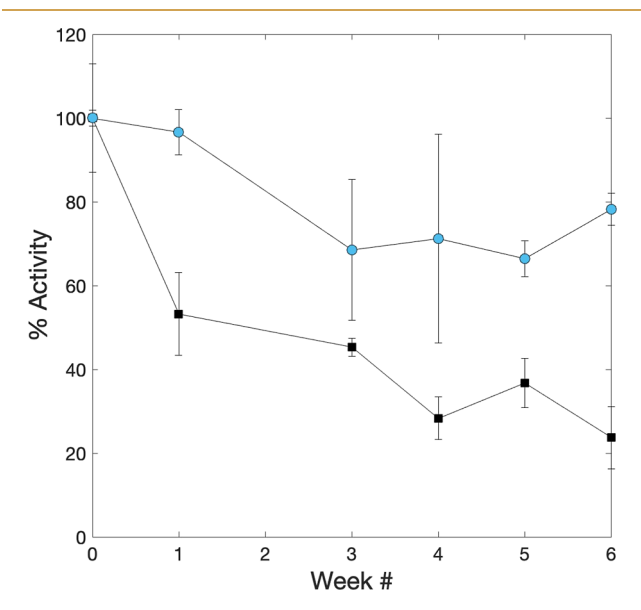


Figure 4. Long-term stability of TrzN:MSN-10 (black squares) and TrzN:MSN-10:Chit (light blue circles) measured over a six-week period. The hydrolysis of 50 μ M atrazine at 25 °C in 50 mM HEPES buffer, pH 7.0, for 1 h. Each biocatalyst was washed and stored at 4 °C in 1 mL of 50 mM HEPES buffer, pH 7.0, and was removed weekly from the storage buffer, decanted, and analyzed.

biomaterial retained 24 \pm 7%, while the TrzN:MSN-10:Chit biomaterial retained 78 \pm 4% of their initial activity. During these experiments, there was no detectable protein loss. The chitosan coating increases the stability of the biocatalyst most likely by preventing the denaturation of amino acids during the storage processes. Remarkably, WT TrzN can also be stored at 4 °C in buffer over a six-week period without significant loss of activity. However, comparison in activity between soluble and immobilized enzymes can be flawed due to the potential distortion of the enzyme from multi-interactions between the enzyme and support. Overall, both biocatalysts showed strong retention of activity during cyclical use over a six-week period with the chitosan coating significantly improving the activity retention of TrzN.

3.5. Stability of TrzN:MSN Biomaterials in Organic Cosolvents

Understanding the ability of the TrzN:MSN-10 biomaterial to function in organic solvents is important in exploring the nanoparticle's overall potential as a bioremediation catalyst. Although atrazine presents itself typically in environments with little to no detectable organic solvents, at higher concentrations atrazine's solubility becomes problematic and requires the addition of organic solvents.³⁹ Additionally, enzymes typically denature when exposed to organic cosolvents.²⁸ Therefore, exploring the activity of the TrzN:MSN-10 and TrzN:MSN-10:Chit biomaterials in organic cosolvents is crucial for establishing them as potential bioremediation catalysts. The activity of TrzN:MSN-10 and TrzN:MSN-10:Chit was examined in MeOH/HEPES buffer, pH 7.0, in ratios of 5:95, 10:90, 20:80, 50:50, 75:25, and 100:0 at 25 °C for 1 h (Figure 5). In 5% MeOH, TrzN:MSN-10 exhibited no

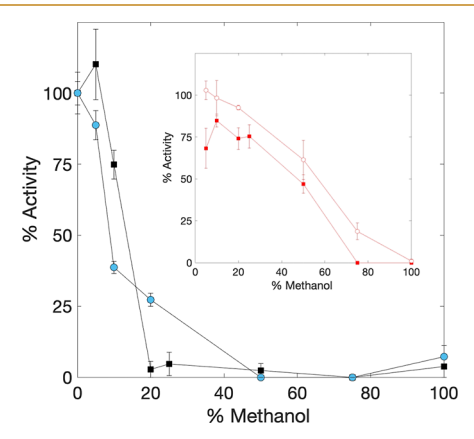


Figure 5. Activity of TrzN:MSN-10 (black squares) and TrzN:MSN-10:Chit (light blue circles) by monitoring the hydrolysis of 50 μ M atrazine at 25 °C in 50 mM HEPES buffer, pH 7.0, for 1 h at varying MeOH concentrations (0–100%). Inset: After reacting with the respective MeOH concentration, TrzN:MSN-10 (red squares) and TrzN:MSN-10:Chit (red-lined circles) were washed and reacted at standard conditions, i.e., 25 °C with 50 μ M atrazine in 50 mM HEPES buffer, pH 7.0, for 1 h.

loss in activity (110 \pm 12%), while the TrzN:MSN-10:Chit biomaterial lost $\sim 10\%$ of its activity (89 \pm 5%). Increasing the MeOH concentration to 10% resulted in a loss of ~25% of the observed activity for the TrzN:MSN-10 biomaterial, while the TrzN:MSN-10:Chit biomaterial lost \sim 60% (39 \pm 2%) of its initial activity. However, in 20% MeOH, the TrzN:MSN-10 biomaterial retained only $3 \pm 2\%$ of its initial activity, while the TrzN:MSN-10:Chit biomaterial retained 27 \pm 3% of its initial activity. For comparison purposes, WT TrzN exhibits ~75% of its native activity in 20% MeOH. 11 It should be noted that enzyme immobilization typically involves new interactions between the enzyme and support, which may alter enzyme conformation, which likely explains the greater loss in activity for immobilized TrzN compared to WT TrzN.31 This new conformation could help explain the higher inhibition of immobilized TrzN compared to soluble TrzN. 11 These data indicate that the TrzN:MSN-10:Chit biomaterial performs best in the presence of MeOH.

Both the TrzN:MSN-10 and TrzN:MSN-10:Chit biomaterials could be partially reactivated after reaction in MeOH/HEPES cosolvent solutions by washing the biomaterials with 50 mM HEPES, pH 7.0 (Figure 5, inset). The washed

biomaterials were reacted with 50 μ M atrazine at 25 $^{\circ}$ C in 50 mM HEPES buffer, pH 7.0, for 1 h revealing that up to 30% MeOH, both biomaterials could be almost fully reactivated. Even at 50:50 MeOH/HEPES, both biomaterials could be reactivated to 47 \pm 6% of their original activity. At higher MeOH concentrations, TrzN:MSN-10:Chit could still be reactivated, but the uncoated TrzN:MSN-10 biomaterial could not. These results suggest that TrzN is not being fully denatured by MeOH, likely due to the stabilization of the protein structure by the biomaterial. Coating the TrzN:MSN-10 biomaterial with chitosan further stabilizes the enzyme structure by "locking" it in place and providing an extra barrier of protection from MeOH. Overall, the TrzN:MSN-10 and TrzN:MSN-10:Chit biomaterials are both active in organic cosolvents, an important finding for bioremediation processes that involve solvent extraction of atrazine from organic soil samples.

3.6. Stability of TrzN:MSN-10 and TrzN:MSN-10:Chit Biomaterials at Nonphysiological pH Values

When utilizing biocatalysts for water bioremediation purposes, the catalyst is expected to be used at the watershed pH, which is typically around pH 7. However, outside influences such as polluted runoff can cause the pH to fluctuate outside of the neutral range. With this in mind, it is important to investigate the activity of TrzN:MSN-10 and TrzN:MSN-10:Chit biomaterials at lower (pH 4.0) and higher (pH 9.0) pH values (Figure 6). At a pH value of 4.0 (50 mM citric acid

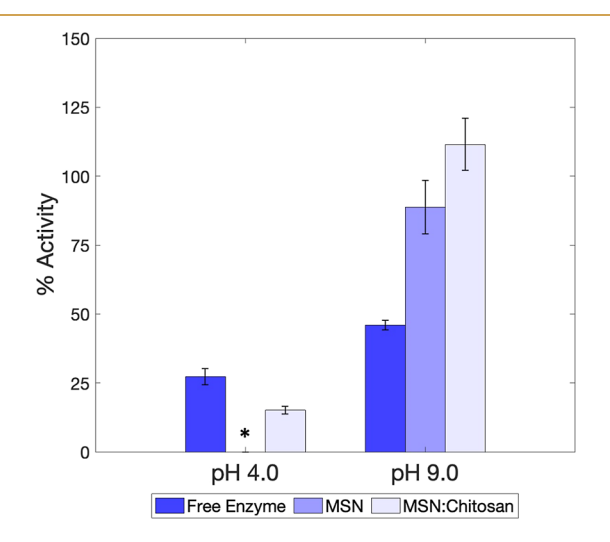


Figure 6. Hydrolysis of 50 μ M atrazine by WT TrzN, TrzN:MSN-10, and TrzN:MSN-10:Chit at 25 °C in 50 mM citric acid buffer, pH 4.0 or 50 mM glycine buffer, pH 9.0 for 1 h. An asterisk indicates that there was no detectable activity.

buffer), the TrzN:MSN-10 biomaterial had no detectable activity, while the TrzN:MSN-10:Chit biomaterial exhibited 15 \pm 1% of its activity at pH 7.0. For comparison purposes, WT TrzN exhibited 27 \pm 3% activity at pH 4.0, a value that is quite similar to that of the TrzN:MSN-10:Chit biomaterial. At a pH value of 9.0 (50 mM glycine buffer), the TrzN:MSN-10 biomaterial exhibited 89 \pm 10% of its activity at pH 7.0, while the TrzN:MSN-10:Chit biomaterial was fully active at 111 \pm 9%. At pH 9.0, both biomaterials outperformed WT TrzN which only exhibited 46 \pm 2% of its activity at pH 7.0. Due to the higher maintained activity at both pH 4.0 and pH 9.0, it can be concluded that coating the TrzN:MSN-10 biomaterial

with chitosan enhances the stability of TrzN at pH values outside of the neutral range.

3.7. Thermostability of TrzN:MSN-10 and TrzN:MSN-10:Chit Biomaterials

The thermostability of the TrzN:MSN-10 and TrzN:MSN-10:Chit biomaterials was evaluated over a temperature range of 50–80 °C using a 30 min heat shock (Figure 7). After heat

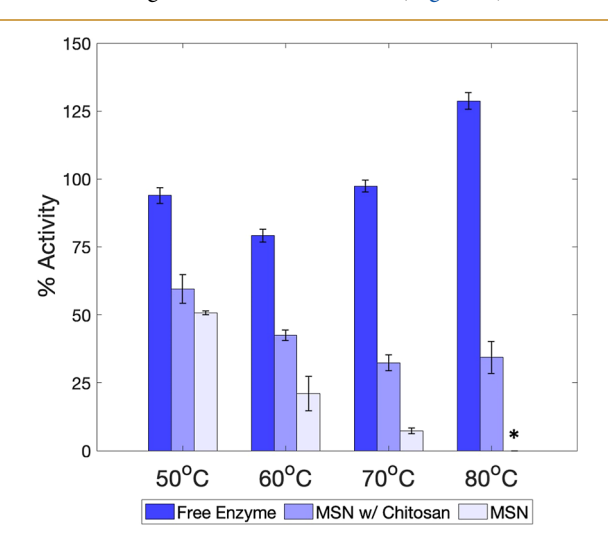


Figure 7. Thermostability of WT TrzN, TrzN:MSN-10, and TrzN:MSN-10:Chit. The specific activity, U/mg, for the hydrolysis of 50 μ M atrazine at 25 °C in 50 mM HEPES buffer, pH 7.0, for 1 h was recorded after a 30 min heat shock at 50, 60, 70, and 80 °C. An asterisk indicates that there was no detectable activity.

shock treatment, the biocatalysts were tested using the standard assay procedure, that is, 50 μM atrazine at 25 $^{\circ}C$ in 50 mM HEPES buffer, pH 7.0. After the 50 °C heat shock, the TrzN:MSN-10 biomaterial retained 50 \pm 1% and the TrzN:MSN-10:Chit biomaterial retained 60 \pm 5% of its original activity. As the temperature was increased, the activities of both biomaterials continued to drop with TrzN:MSN-10 exhibiting 21 \pm 6, 7 \pm 1, and 0% of its original activity at 60, 70, and 80 °C, respectively. The chitosan coating provided additional thermal protection for TrzN with the TrzN:MSN-10:Chit biomaterial exhibiting 43 ± 2 , 32 ± 3 , and $34 \pm 6\%$ of its original activity at 60, 70, and 80 °C. For comparison purposes, WT TrzN retains >80% of its original activity after a 50, 60, 70, and 80 °C heat shock. The decrease in activity in the biocatalysts compared to the soluble enzyme is likely due to the interactions that immobilize TrzN to the material, which restricts the essential motion of the folded state that is required for catalytic turnover. 41 This has been observed before in multipoint covalent immobilization methods. The chitosan coating stabilizes TrzN bound to MSN-10 at higher temperatures, which is consistent with previous studies where chitosan coatings have been shown to increase the thermostability of immobilized enzymes. 11,35

3.8. Activity of TrzN:MSN-10 and TrzN:MSN-10:Chit Biomaterials in River Water

The commercial bioremediation application of any biomaterial requires that it retains its desired catalytic activity in river or lake water. To replicate these conditions, water samples were collected from Clear Creek in Golden, Colorado. There was no reported atrazine contamination in Clear Creek according to the most recent water quality report published by the City of

Golden in 2022. 42 The sample had an initial temperature of 3 $^{\circ}$ C and a pH of 7.25. Two sample sets were prepared; the first (group 1) was unmodified, while the second (group 2) was autoclaved. Aliquots from group 1 were plated on agar plates and incubated at 37 $^{\circ}$ C. Bacterial growth was observed after 48 h (S12, Supporting Information). Because atrazine is not present in Clear Creek, all samples were supplemented with 15 mM atrazine in 100% MeOH providing an atrazine concentration of 50 μ M and final MeOH concentrations of <1%. All samples were run at 25 $^{\circ}$ C with 200 rpm stirring for 1 h. These data indicated that both the TrzN:MSN-10 and TrzN:MSN-10:Chit biomaterials retain full activity under field conditions. In addition to being fully functional, MSN-10 is a biocompatible material that is suitable for commercial bioremediation purposes.

4. CONCLUSIONS

In summary, TrzN was immobilized on nonfunctionalized and Zn(II)-functionalized MSNs with different pore sizes: MCM-41 (small, 3 nm), MSN-10 (medium, 6-12 nm), and PEMSN-10 (large, 15-30 nm). Each of these MSNs bound TrzN and was capable of catalytically hydrolyzing atrazine at pH 7 and 25 °C. The MSN support system with the highest TrzN activity was MSN-10 (TrzN:MSN-10), which became the focus of this study with and without a protective chitosan coating (TrzN:MSN-10:Chit). Coating the TrzN:MSN-10 biomaterial with chitosan did not reduce the observed activity but was shown to provide enhanced stability of TrzN improving reusability, organic solvent, thermal, and pH stability. Both TrzN:MSN-10 and TrzN:MSN-10:Chit could be cyclically reused over five consecutive cycles in several storage conditions, remaining active for at least 6 weeks. TrzN:MSN-10:Chit was superior to TrzN:MSN-10 as it exhibited higher activity under all storage conditions with >60% activity retained. TrzN:MSN-10:Chit was superior to TrzN:MSN-10 in the presence of 20% MeOH, low (pH 4) and high (pH 9) values, and high temperatures up to 80 °C. Therefore, the TrzN:MSN-10:Chit biomaterial exhibited the best overall profile making this TrzN biomaterial a promising biocatalyst for the bioremediation of atrazine by dechlorination. The fact that TrzN:MSN-10:Chit was fully active in river water establishes it as a functional biomaterial under actual field conditions.

ASSOCIATED CONTENT

Supporting Information

The Supporting Information is available free of charge at https://pubs.acs.org/doi/10.1021/acsenvironau.3c00036.

Additional material characterization, N_2 sorption, TEM, ICP, TGA, and SEM; 3D PyMOL image of TrzN; additional long-term stability data; and images of bacterial growth on the unmodified Clear Creek samples (PDF)

AUTHOR INFORMATION

Corresponding Authors

Richard C. Holz – Department of Chemistry, Colorado School of Mines, Golden, Colorado 80401, United States; Quantitative Biosciences and Engineering Program, Colorado School of Mines, Golden, Colorado 80401, United States; orcid.org/0000-0001-6093-2799; Email: Rholz@mines.edu

Brian G. Trewyn — Department of Chemistry, Colorado School of Mines, Golden, Colorado 80401, United States; National Renewable Energy Laboratory, Golden, Colorado 80401, United States; Materials Science Program, Colorado School of Mines, Golden, Colorado 80401, United States; orcid.org/0000-0003-4027-7402; Email: Btrewyn@ mines.edu

Authors

Karla Diviesti — Quantitative Biosciences and Engineering Program, Colorado School of Mines, Golden, Colorado 80401, United States

Glory A. Russell-Parks — Department of Chemistry, Colorado School of Mines, Golden, Colorado 80401, United States;
ocid.org/0000-0001-9059-1681

Complete contact information is available at: https://pubs.acs.org/10.1021/acsenvironau.3c00036

Author Contributions

Leaves authorship, K.D and G.A.R.-P contributed equally to this paper. CRediT:Karla Diviesti data curation, formal analysis, investigation, writing-original draft; Glory A. Russell-Parks data curation, formal analysis, investigation, writing-review & editing; Brian G. Trewyn conceptualization, methodology, project administration, supervision, writing-review & editing; Richard C Holz conceptualization, formal analysis, funding acquisition, project administration, supervision, writing-review & editing.

Funding

This work was supported by the National Science Foundation (CHE-2003861, RCH) and the National Institution of Health (1R15CA271365, BGT).

Notes

The authors declare no competing financial interest.

REFERENCES

- (1) de Albuquerque, F. P.; de Oliveira, J. L.; Moschini-Carlos, V.; Fraceto, L. F. An Overview of the Potential Impacts of Atrazine in Aquatic Environments: Perspectives for Tailored Solutions Based on Nanotechnology. *Sci. Total Environ.* **2020**, *700*, 134868.
- (2) Solomon, K. R.; Baker, D. B.; Richards, R. P.; Dixon, K. R.; Klaine, S. J.; La Point, T. W.; Kendall, R. J.; Weisskopf, C. P.; Giddings, J. M.; Giesy, J. P.; Hall, L. W.; Williams, W. M. Ecological risk assessment of atrazine in North American surface waters. *Environ. Toxicol.* **1996**, *15* (1), 31–76.
- (3) Beaulieu, M.; Cabana, H.; Taranu, Z.; Huot, Y. Predicting Atrazine Concentrations in Waterbodies across the Contiguous United States: The Importance of Land Use, Hydrology, and Water Physicochemistry. *Limnol. Oceanogr.* **2020**, *65*, 2966–2983.
- (4) Ocking, D. A. J. H.; Abbitt, K. I. J. B. Amphibian Contributions to Ecosystem Services. *Herpetol. Conserv. Biol.* **2014**, *9*, 1–17.
- (5) Hayes, T. B.; Khoury, V.; Narayan, A.; Nazir, M.; Park, A.; Brown, T.; Adame, L.; Chan, E.; Buchholz, D.; Stueve, T.; Gallipeau, S. Atrazine Induces Complete Feminization and Chemical Castration in Male African Clawed Frogs (Xenopus Laevis). *Proc. Natl. Acad. Sci. U.S.A.* **2010**, *107* (10), 4612–4617.
- (6) Liu, Z.; Wang, Y.; Zhu, Z.; Yang, E.; Feng, X.; Fu, Z.; Jin, Y. Atrazine and Its Main Metabolites Alter the Locomotor Activity of Larval Zebrafish (Danio Rerio). *Chemosphere* **2016**, *148*, 163–170.
- (7) Pathak, R. K.; Dikshit, A. K. Atrazine and Human Health. *Int. J. Ecosys.* **2012**, *1* (1), 14–23.

- (8) Rostami, S.; Jafari, S.; Moeini, Z.; Jaskulak, M.; Keshtgar, L.; Badeenezhad, A.; Azhdarpoor, A.; Rostami, M.; Zorena, K.; Dehghani, M. Current Methods and Technologies for Degradation of Atrazine in Contaminated Soil and Water: A Review. *Environ. Technol. Innov.* **2021**, *24*, 102019.
- (9) Li, Q.; Li, Y.; Zhu, X.; Cai, B. Isolation and Characterization of Atrazine-Degrading Arthrobacter Sp. AD26 and Use of This Strain in Bioremediation of Contaminated Soil. *J. Environ. Sci.* **2008**, 20 (10), 1226–1230.
- (10) Sheldon, R. A. Enzyme Immobilization: The Quest for Optimum Performance. *Adv. Synth. Catal.* **2007**, 349 (8–9), 1289–1307.
- (11) Diviesti, K.; Holz, R. C. Catalytic Biomaterials for Atrazine Degradation. *Catalysts* **2023**, *13* (1), 140.
- (12) Lin, J.; Brown, C. W. Sol-Gel Glass as a Matrix for Chemical and Biochemical Sensing. *TrAC, Trends Anal. Chem.* **1997**, *16* (4), 200–211.
- (13) Yang, B.; Tang, K.; Wei, S.; Zhai, X.; Nie, N. Preparation of Functionalized Mesoporous Silica as a Novel Carrier and Immobilization of Laccase. *Appl. Biochem. Biotechnol.* **2021**, *193* (8), 2547–2566.
- (14) Wang, Y.; Caruso, F. Mesoporous Silica Spheres as Supports for Enzyme Immobilization and Encapsulation. *Chem. Mater.* **2005**, *17* (5), 953–961.
- (15) Narayan, R.; Nayak, U. Y.; Raichur, A. M.; Garg, S. Mesoporous Silica Nanoparticles: A Comprehensive Review on Synthesis and Recent Advances. *Pharmaceutics* **2018**, *10* (3), 118–149.
- (16) Pei, X.; Luo, Z.; Qiao, L.; Xiao, Q.; Zhang, P.; Wang, A.; Sheldon, R. A. Putting Precision and Elegance in Enzyme Immobilisation with Bio-Orthogonal Chemistry. *Chem. Soc. Rev.* **2022**, *51* (16), 7281–7304.
- (17) López-Laguna, H.; Sánchez, J. M.; Carratalá, J. V.; Rojas-Peña, M.; Sánchez-García, L.; Parladé, E.; Sánchez-Chardi, A.; Voltà-Durán, E.; Serna, N.; Cano-Garrido, O.; Flores, S.; Ferrer-Miralles, N.; Nolan, V.; de Marco, A.; Roher, N.; Unzueta, U.; Vazquez, E.; Villaverde, A. Biofabrication of Functional Protein Nanoparticles through Simple His-Tag Engineering. ACS Sustain. Chem. Eng. 2021, 9 (36), 12341–12354.
- (18) Chen, C.-Y.; Li, H.-X.; Davis, M. E. Studies on Mesoporous Materials. *Microporous Mater.* **1993**, 2 (1), 17–26.
- (19) Valenstein, J. S.; Kandel, K.; Melcher, F.; Slowing, I. I.; Lin, V. S. Y.; Trewyn, B. G. Functional Mesoporous Silica Nanoparticles for the Selective Sequestration of Free Fatty Acids from Microalgal Oil. ACS Appl. Mater. Interfaces 2012, 4 (2), 1003–1009.
- (20) Schweitzer, N. M.; Hu, B.; Das, U.; Kim, H.; Greeley, J.; Curtiss, L. A.; Stair, P. C.; Miller, J. T.; Hock, A. S. Propylene Hydrogenation and Propane Dehydrogenation by a Single-Site Zn2+ on Silica Catalyst. *ACS Catal.* **2014**, *4* (4), 1091–1098.
- (21) Shapir, N.; Pedersen, C.; Gil, O.; Strong, L.; Seffernick, J.; Sadowsky, M. J.; Wackett, L. P. TrzN from Arthrobacter Aurescens TC1 Is a Zinc Amidohydrolase. *J. Bacteriol.* **2006**, *188* (16), 5859–5864
- (22) Mu, Y.; Zhan, G.; Huang, C.; Wang, X.; Ai, Z.; Zou, J.; Luo, S.; Zhang, L. Dechlorination-Hydroxylation of Atrazine to Hydroxyatrazine with Thiosulfate: A Detoxification Strategy in Seconds. *Environ. Sci. Technol.* **2019**, 53 (6), 3208–3216.
- (23) Jackson, C. J.; Coppin, C. W.; Carr, P. D.; Aleksandrov, A.; Wilding, M.; Sugrue, E.; Ubels, J.; Paks, M.; Newman, J.; Peat, T. S.; Russell, R. J.; Field, M.; Weik, M.; Oakeshott, J. G.; Scott, C. 300-Fold Increase in Production of the Zn2+-Dependent Dechlorinase TrzN in Soluble Form via Apoenzyme Stabilization. *Appl. Environ. Microbiol.* **2014**, *80* (13), 4003–4011.
- (24) Seffernick, J. L.; Reynolds, E.; Fedorov, A. A.; Fedorov, E.; Almo, S. C.; Sadowsky, M. J.; Wackett, L. P. X-Ray Structure and Mutational Analysis of the Atrazine Chlorohydrolase TrzN. *J. Biol. Chem.* **2010**, 285 (40), 30606–30614.
- (25) Gaffney, D. A.; O'Neill, S.; O'Loughlin, M. C.; Hanefeld, U.; Cooney, J. C.; Magner, E. Tailored Adsorption of His6-Tagged Protein onto Nickel(Ii)-Cyclam Grafted Mesoporous Silica. *Chem. Commun.* **2010**, *46* (7), 1124–1126.

- (26) Heidari, R.; Khosravian, P.; Mirzaei, S. A.; Elahian, F. SiRNA Delivery Using Intelligent Chitosan-Capped Mesoporous Silica Nanoparticles for Overcoming Multidrug Resistance in Malignant Carcinoma Cells. *Sci. Rep.* **2021**, *11* (1), 20531–20614.
- (27) Seffernick, J. L.; Reynolds, E.; Fedorov, A. A.; Fedorov, E.; Almo, S. C.; Sadowsky, M. J.; Wackett, L. P. X-Ray Structure and Mutational Analysis of the Atrazine Chlorohydrolase TrzN. *J. Biol. Chem.* **2010**, 285 (40), 30606–30614.
- (28) Martinez, S.; Kuhn, M. L.; Russell, J. T.; Holz, R. C.; Elgren, T. E. Acrylamide Production Using Encapsulated Nitrile Hydratase from Pseudonocardia Thermophila in a Sol-Gel Matrix. *J. Mol. Catal. B: Enzym.* **2014**, *100*, 19–24.
- (29) Thommes, M.; Kaneko, K.; Neimark, A. V.; Olivier, J. P.; Rodriguez-Reinoso, F.; Rouquerol, J.; Sing, K. S. W. Physisorption of Gases, with Special Reference to the Evaluation of Surface Area and Pore Size Distribution (IUPAC Technical Report). *Pure Appl. Chem.* **2015**, *87* (9–10), 1051–1069.
- (30) Szymańska, E.; Winnicka, K. Stability of Chitosan A Challenge for Pharmaceutical and Biomedical Applications. *Mar. Drugs* **2015**, *13* (4), 1819–1846.
- (31) Garcia-Galan, C.; Berenguer-Murcia, A.; Fernandez-Lafuente, R.; Rodrigues, R. C. Potential of Different Enzyme Immobilization Strategies to Improve Enzyme Performance. *Adv. Synth. Catal.* **2011**, 353 (16), 2885–2904.
- (32) Darby, J. F.; Atobe, M.; Firth, J. D.; Bond, P.; Davies, G. J.; O'Brien, P.; Hubbard, R. E. Increase of Enzyme Activity through Specific Covalent Modification with Fragments. *Chem. Sci.* **2017**, 8 (11), 7772–7779.
- (33) Lee, K. Y.; Mooney, D. J. Alginate: Properties and Biomedical Applications. *Prog. Polym. Sci.* **2012**, *37* (1), 106–126.
- (34) Bedade, D. K.; Sutar, Y. B.; Singhal, R. S. Chitosan Coated Calcium Alginate Beads for Covalent Immobilization of Acrylamidase: Process Parameters and Removal of Acrylamide from Coffee. *Food Chem.* **2019**, 275, 95–104.
- (35) Fareez, I. M.; Lim, S. M.; Mishra, R. K.; Ramasamy, K. Chitosan Coated Alginate-Xanthan Gum Bead Enhanced PH and Thermotolerance of Lactobacillus Plantarum LAB12. *Int. J. Biol. Macromol.* **2015**, 72, 1419–1428.
- (36) Lohiya, G.; Katti, D. S. Carboxylated Chitosan-Mediated Improved Efficacy of Mesoporous Silica Nanoparticle-Based Targeted Drug Delivery System for Breast Cancer Therapy. *Carbohydr. Polym.* **2022**, 277, 118822.
- (37) Ning, C.; Jiajia, J.; Meng, L.; Hongfei, Q.; Xianglong, W.; Tingli, L. Electrophoretic Deposition of GHK-Cu Loaded MSN-Chitosan Coatings with PH-Responsive Release of Copper and Its Bioactivity. *Mater. Sci. Eng., C* **2019**, *104* (May), 109746.
- (38) Chiang, Y. W.; Wang, T. H.; Lee, W. C. Chitosan Coating for the Protection of Amino Acids That Were Entrapped within Hydrogenated Fat. *Food Hydrocolloids* **2009**, 23 (3), 1057–1061.
- (39) Im, J. K.; Cho, Y. C.; Noh, H. R.; Yu, S. J. Geographical Distribution and Risk Assessment of Volatile Organic Compounds in Tributaries of the Han River Watershed. *Agronomy* **2021**, *11* (5), 956.
- (40) Baker, J. P.; Bernard, D. P.; Christensen, S. W.; Sale, M. J.; Freda, J.; Heltcher, K.; Marmorek, D.; Rowe, L.; Scanlon, P.; Suter, G.; Warren-Hicks, W. J.; Welbourn, P. M. Biological Effects of Changes in Surface Water Acid-Base Chemistry, Acidic Deposition: State of Science and Technology; National Acid Precipitation Assessment Program, 1990.
- (41) Weltz, J. S.; Kienle, D. F.; Schwartz, D. K.; Kaar, J. L. Reduced Enzyme Dynamics upon Multipoint Covalent Immobilization Leads to Stability-Activity Trade-Off. *J. Am. Chem. Soc.* **2020**, *142* (7), 3463–3471.
- (42) City of Golden Public Works Department. 2022 Water Quality Report: Golden, 2022. www.cityofgolden.net/DrinkingWater (accessed Aug 13, 2023).